Int. J. Environ. Sci. Technol.
DOI 10.1007/s13762-016-1214-x

ORIGINAL PAPER

The relationship between molecular composition and fluorescence properties of humic substances

M. Ateia[1] · J. Ran[1] · M. Fujii[1] · C. Yoshimura[1]

Received: 31 May 2016 / Revised: 18 October 2016 / Accepted: 20 December 2016

Abstract The quantity and quality of dissolved organic matters have been widely characterized by fluorescence spectroscopy, yet the relationship between the fluorescence properties of dissolved organic matters and its molecular composition remains poorly described in the literature. Here, we measured the fluorescence excitation–emission matrix of 17 well-characterized humic substance standards to determine a range of fluorescence parameters, including classical fluorescence indices (e.g., fluorescence index, biological index and humification index) and parameters derived from parallel factor analysis (e.g., component contribution). Relationships between humic substance's fluorescence and compositional parameters were then statistically examined using canonical correspondence and simple correlation analyses. The canonical correspondence analysis generally suggested that most fluorescence parameters determined here are highly associated with the amount of aliphatic and aromatic compounds in humic substances. However, the correlation analysis between single molecular and fluorescence parameters indicated that the fluorescence properties of humic substances including the parallel factor analysis component contribution also significantly correlate well with several aspects of the molecular composition of humic substances, such as elemental composition, carbon species, acidic functional group and iron complexation. Overall, our results suggest that measurement of humic substance's fluorescence is beneficial in understanding the molecular composition and environmental functions of dissolved organic matters in natural and engineered waters.

Keywords Humic substances · Fluorescence index · Molecular composition · Parallel factor analysis · Excitation Emission Matrix · Iron complexation

Introduction

Humic substances (HSs) represent a major carbon reservoir in the biosphere and comprise a heterogeneous macromolecular assembly of diverse small components stabilized by hydrophobic interactions and hydrogen bonds (Piccolo 2001). In natural and engineered aqueous systems, HS accounts for up to 80% of dissolved organic matter (DOM) (Aiken 1985). Because HS is heterogeneous, HS quality is typically described using parameters such as elemental composition/ratio, carbon species, functional groups and other parameters, depending on the purpose of the study (Campitelli et al. 2006; Chin et al. 1994).

Most information on the molecular composition of HS is typically associated with its environmental and ecological functions; consequently, the characterization of compositional parameters is important for understanding the biogeochemical processes of HS in aqueous matrices (Hertkorn et al. 2006; Schmidt et al. 2009). For example, previous studies have indicated that HS with a high proportion of aromatic compounds (which are π-electron carriers) generally has a higher capacity of ultraviolet and visible (UV–Vis) radiation absorbance (Bukaveckas and Robbins-Forbes 2000; Schindler et al. 1996), functions as an electron shuttle (Scott et al. 1998) and produces reactive oxygen species (Scully et al. 2003). Other functional

Editorial responsibility: M. Abbaspour.

✉ M. Fujii
fujii.m.ah@m.titech.ac.jp

[1] Department of Civil Engineering, Tokyo Institute of Technology, 2-12-1-M1-4 Ookayama, Tokyo 152-8552, Japan

Published online: 02 January 2017

groups, such as carboxyl and phenolic hydroxyl groups, are responsible for metal complexation and alkalinity (Sundman et al. 2013; Tipping et al. 2002).

Spectrophotometric techniques, including fluorescence and UV–Vis absorbance measurements, have been widely used to characterize aqueous DOM. These optical techniques have the distinct advantages of being rapid, simple and relatively inexpensive to perform and thus are often incorporated into routine monitoring systems. Measurements of DOM fluorescence indices, including fluorescence index (FI) (McKnight et al. 2001), biological index (BIX) (Huguet et al. 2009) and humification index (HIX) (Zsolnay et al. 1999), can provide practical information such as the source of the DOM and its chemical and biological reactivity (Coble 1996; Jaffé et al. 2008; McKnight et al. 2001). In addition, fluorescence excitation–emission matrix combined with parallel factor (EEM-PARAFAC) analysis is now widely available. The analytical procedure of EEM-PARAFAC is, for example, described in a tutorial by Stedmon and Bro (2008)). The EEM-PARAFAC analysis can decompose three-dimensional EEM maps from a large set of samples into a smaller number of individual fluorescent components such as terrestrial and marine humic- and protein-like groups (Baghoth et al. 2011; Stedmon et al. 2007). Thus, this analysis may allow for more comprehensive data interpretation than do classical peak-picking and other monotonicity-based analytical approaches involving a relatively small number of samples.

Fluorescence techniques have been developed and applied for characterization and structural evaluation of humic substances. However, the relationship between the fluorescence indices and the molecular properties of HS was not emphasized due to the limited number of HS types employed in previous reported works (Minor and Stephens 2008; Rodríguez et al. 2014). In this article, we examined the relationship between EEM-derived parameters and the molecular composition and functional parameters of totally 17 standard HS. We have carefully investigated the relevance of HS fluorescence to its molecular composition and gave useful practical implications from the findings of our study. The experiments were performed, and data were analyzed during the period between 2014 and 2015 at the Department of Civil and Environmental Engineering, Tokyo Institute of Technology, Japan.

Materials and methods

General

The chemicals used in this work were stored according to the manufacturers' instructions and were used as received. Stock solutions and sample solutions were prepared using ultra-pure Milli-Q water (MQ, Millipore, resistivity of 18 MΩ cm at 25 °C). All plasticware and glassware were acid-washed by soaking in 5% nitric acid for several days, rinsed with MQ and dried prior to use. All solutions used for experiments were adjusted to 25 °C in a water bath before use. All measurements were taken in a temperature-controlled room at 25 °C.

Solution pH was measured using a HM25R pH meter (TOA DKK, Japan) equipped with a combined electrode (1.2 mm diameter, GST-5731C). The pH meter was calibrated against phthalate and phosphate pH standards (TOA DKK) adjusted to pH 4.01 ± 0.02 and 6.86 ± 0.02 at 25 °C, respectively, according to the JIS Z8802 pH measurement method. The pH of the solutions was adjusted using 1–5 M hydrochloric acid (HCl) and sodium hydroxide (NaOH) solutions prepared by diluting 36% (w/v) concentrated HCl (Kanto Chemical Co. Inc., Japan) and by dissolving NaOH (Kanto Chemical), respectively.

Seventeen chemically well-defined HS standards were purchased from the International Humic Substances Society (IHSS) and the Japanese Humic Substances Society (JHSS). The chemical properties of these HS standards, including elemental composition/ratio, carbon species, the concentration of acidic functional groups and iron complexation parameters, are listed in Table 1. Lyophilized HS samples (5–10 mg) were accurately weighed into 1.5 mL polypropylene microtubes using a Sartorius microbalance (ME5, Germany) with ±1 μg readability and then dissolved in an appropriate volume of 0.01–0.1 M NaOH solution (depending on HS solubility) to provide 10 g L^{-1} HS stock solution. The pH of each HS solution was adjusted to 8.0 ± 0.2 with HCl or NaOH, as described above. The volume of acid or alkali solution required for each adjustment was recorded (generally less than about 50 μL); the volume increase during the pH adjustment was <10% of the initial volume and was taken into account during calculation of the final HS concentration in the HS stock solution. Each HS stock solution was diluted with bicarbonate ($NaHCO_3$) buffer (pH 8.0 ± 0.05) to provide a 5-mg L^{-1} test HS solution. Photochemical transformation of HS was prevented by minimizing exposure of the HS stock solution to room light during pH adjustment and other processes in the stock preparation by placing the samples in a cardboard box when not in use.

EEM data collection

Fluorescence EEM spectra were collected using a RF-5300 fluorescence spectrometer (Shimadzu Co. Ltd., Japan) and a quartz cuvette (1 cm path length). The measured wavelength range was from 240 to 450 nm for excitation (Ex: at 5-nm intervals) and from 300 to 600 nm for emission (Em: at 2-nm intervals). Prior to each measurement, the

Table 1 Chemical properties of humic substances used in this study

Fraction	Code	Origin	Elemental composition (%)[e]					Elemental ratio			Carbon species from ^{13}C NMR (%)				Aroma-ticity[d]	Acidic functional groups (meq/g)		Fe(III) complexation parameters[f]	
			C	H	O	N	S	O/C	N/C	H/C	Aliphatic	Carbohydrate	Aromatic	Carbonyl		Carboxyl	Phenolic	K_{FeL} ($\times 10^{11}$ M^{-1})	C_{Fe} ($\times 10^{-8}$ mol mg^{-1})
FA	1R105F	Nordic Lake[a]	52	4.0	45	0.68	0.46	0.65	0.011	0.91	18	19.0	31	34	0.46	5.84	1.66	1.77	4.79
	1R109F	Pony Lake[a]	52	5.4	31	6.50	3.00	0.45	0.106	1.20	61	8.6	12	18	0.15	ND[g]	ND[g]	14.4	0.49
	1S101F	Suwanne River I[a]	52	4.3	42	0.72	0.44	0.60	0.012	0.98	33	16.0	24	27	0.33	6.00	1.53	0.31	6.56
	2S101F	Suwanne River II[a]	52	4.4	43	0.67	0.46	0.62	0.011	0.99	35	22.0	22	22	0.28	5.85	1.49	1.01	3.34
	2S103F	Pahokee Peat II[a]	51	3.5	43	2.34	0.76	0.63	0.039	0.82	ND[g]	ND[g]	ND[g]	ND[g]	ND[g]	ND[g]	ND[g]	ND[g]	ND[g]
	IFA	Inogashira Soil[b]	43	3.5	21	1.70	0.08	0.89	0.034	0.96	26	16.0	27	30	0.39	9.81	1.07	0.96	1.88
	DFA	Dado Soil[b]	48	3.5	48	0.77	0.01	0.76	0.014	0.88	22	19.0	37	22	0.48	7.72	1.36	2.10	4.03
	BFA	Biwa Lake[c]	56	6.1	36	ND[g]	ND[g]	0.47	0.041	1.30	39	24.0	17	20	0.21	ND[g]	ND[g]	2.17	0.21
HA	1R103H	Pahokee Peat II[a]	57	3.6	37	3.70	0.70	0.48	0.056	0.75	ND[g]	ND[g]	ND[g]	ND[g]	ND[g]	ND[g]	ND[g]	ND[g]	ND[g]
	1R105H	Nordic Lake[a]	43	4.0	43	1.20	0.58	0.61	0.019	0.89	15	18.0	38	29	0.54	4.83	1.72	0.64	6.51
	1R107H	Waskish Peat[a]	55	4.0	39	1.50	0.36	0.53	0.023	0.88	18	14.0	42	26	0.57	ND[g]	ND[g]	1.86	6.12
	1S102H	Elliott Soil[a]	58	3.7	34	4.10	0.44	0.44	0.061	0.75	16	10.0	50	24	0.66	4.81	1.09	1.01	23.7
	1S103H	Pahokee Peat II[a]	56	3.8	37	3.70	0.71	0.50	0.056	0.81	19	9.0	47	25	0.63	5.08	1.08	1.52	8.40
	1S104H	Leonardite[a]	64	3.7	31	1.20	0.76	0.37	0.017	0.69	14	5.0	58	23	0.75	4.76	1.47	1.59	15.6
	2S101H	Suwannee River II[a]	53	4.3	42	1.20	0.54	0.60	0.019	0.97	29	20.0	31	21	0.39	7.81	1.96	1.22	3.96
	IHA	Inogashira Soil[b]	55	4.3	37	4.00	0.26	0.50	0.063	1.20	22	22.0	37	19	0.45	4.35	1.96	5.27	5.20
	DHA	Dando Soil[b]	53	5.3	37	4.50	0.29	0.52	0.073	0.93	30	23.0	33	14	0.38	3.70	2.18	1.54	8.82

[a] International Humic Substances Society

[b] Japanese Humic Substances Society (Watanabe et al. 1994)

[c] Japanese Humic Substances Society (Fujitake et al. 2009)

[d] Aromaticity was determined from aromatic carbon (%)/[aromatic carbon (%) + carbohydrate (%) + aliphatic carbon (%)]

[e] Mass ratio (%)

[f] Conditional stability constant (K_{FeL}) and complexation capacity (C_{Fe}) for Fe(III) at pH 8. Values reported by Fujii et al. (2014))

[g] Values not determined

spectrometer was auto-zeroed with MQ in the cuvette. Fluorescence signals were recorded as Raman units rather than quinine sulfate units. Raman scans were obtained at Ex = 350 nm at 2-nm emission intervals to calculate the Raman peak areas. Routine data pre-treatment procedures, including spectral correction, inner filter correction, Raman normalization and blank subtraction, were performed according to the procedure described elsewhere (Murphy et al. 2010).

Classical fluorescence indices

Conventional EEM indices were determined as follows: FI was calculated by the ratio of the emission intensity at Em 450 nm relative to that at Em 500 nm against Ex 370 nm (McKnight et al. 2001). BIX was calculated by taking the intensity ratio of Em 380 nm relative to that of Em 430 nm against Ex 310 nm (Huguet et al. 2009). HIX was determined from the ratio of two integrated regions of the emission scans (Em 435–480 nm divided by Em 300–345 nm at Ex 254 nm) (Zsolnay et al. 1999).

PARAFAC modeling

PARAFAC modeling was conducted following EEM data correction and management proposed by Stedmon and Bro (Stedmon and Bro 2008). The EEM data set was decomposed into trilinear terms plus a residual matrix, thus allowing PARAFAC to estimate the underlying EEM spectra by minimizing the sum of the squared residual of the model.

$$I_{ijk} = \sum_{n=1}^{N} a_{in} b_{jn} c_{kn} + \varepsilon_{ijk}, \quad (1)$$

where I_{ijk} is the intensity of fluorescence for the i-th sample at the j-th emission wavelength and the k-th excitation wavelength, a_{in} is defined as scores and is correlated with the concentration of the n-th component in the i-th sample, b_{jn} and c_{kn} are estimates of the emission and excitation spectral loadings, respectively, for the n-th component, N indicates the number of components in the model, and ε_{ijk} is defined as the residual element which is not accounted for by the model. The model was calculated by minimizing the sum of squared residuals with an alternating least squares algorithm. The MATLAB "FDOMcorrect" toolbox was used for EEM data pre-treatment and the "DOMFluor" toolbox was used to perform the PARAFAC analyses. The PARAFAC analysis was validated, and the most appropriate number of components was determined by residual analysis, split-half analysis and core consistency determination (Stedmon et al. 2003). Previous studies have also successfully employed PARAFAC analysis with the sample number comparable to that used in this study (Carstea et al. 2014; Ferretto et al. 2014). The PARAFAC model provides component scores and loadings. In this procedure, the intensity of the n-th component (I_n) can be calculated by the following equation (Kowalczuk et al. 2009):

$$I_n = \text{Score}_n \cdot \text{Ex}_n(\lambda_{\max}) \cdot \text{Em}_n(\lambda_{\max}), \quad (2)$$

where Score_n is the relative intensity of the n-th component, Ex_n ($\lambda_{\max}$) is the maximum excitation loading of the n-th component, and Em_n ($\lambda_{\max}$) is the maximum emission loading of the n-th component derived from the PARAFAC model. The total fluorescence intensity of a given sample (I_{TOT}) was calculated as the total sum of components, as described below:

$$I_{\text{TOT}} = \sum_{n=1}^{N} I_n \quad (3)$$

The contribution of the n-th component relative to the total fluorescence intensity ($I_n\%$) was then calculated by the following equation:

$$I_n\% = \frac{I_n}{I_{\text{TOT}}} \quad (4)$$

The relative fluorescence intensity (RF_m) was calculated as

$$\text{RF}_m = \frac{P_m}{\sum_{m=1}^{M} P_m} \quad (5)$$

where P_m is the intensity of a specific peak chosen by PARAFAC, M is the total number of peaks derived from PARAFAC analysis, and RF represents the relative intensity of the peak in EEM (the subscript m represents the number of specific peaks). $I_n\%$ is calculated using statistically derived parameters such as scores and loadings, and RF_m is calculated based on the specific peak intensity chosen by PARAFAC modeling.

Other statistical analyses

Statistical analyses, including t test, regression analysis and correlation analysis, were performed using the statistical software R (version 3.1.0). Additionally, canonical correspondence analysis (CCA) was performed using PC-ORD (version 5) software on the Windows platform.

Results and discussion

Fluorescence EEM spectra

Two main peaks in addition to Rayleigh scattering signals (Peiris et al. 2011) were observed in the EEM spectra of all

17 HS standards (Fig. 1). The first peak located in the UV region [excitation wavelength (Ex) ~ 250 nm] was defined previously as peak A (Coble 1996) or peak α (Parlanti et al. 2000). The second peak located in the visible region of the spectrum (Ex ~ 330 nm) has been previously defined as peak C (Coble 1996) or peak α′ (Parlanti et al. 2000). Peak A appeared at about Ex 250 nm in the current study, consistent with the findings of Sierra et al. (2005)) and Peiris et al. (2011)), whereas other studies observed peak A at a slightly lower wavelength (Ex ~ 220 nm) (Alberts et al. 2002; Stedmon et al. 2003). This discrepancy in peak excitation wavelength is likely attributed to the range of wavelengths employed in this study and studies by Sierra et al. (2005)) and Peiris et al. (2011)) and the wavelengths used in the latter studies: the lowest excitation wavelength employed in the former studies was 240 nm, while the latter studies used about 220 nm.

The excitation and emission (Ex/Em) wavelengths of peaks A and C for the 17 HS standards examined here were generally comparable to those reported in the literature (Table 2). We found a significant positive correlation between aromaticity and emission peak wavelength of the 15 HS standards for which aromaticity data are available ($r = 0.75$ and $p = 0.0012$ for peak A and $r = 0.74$ and $p = 0.0015$ for peak C, Fig. 3B. The observed peak shift is likely due to the redshift of fluorescence peaks associated with HS molecular conjugation (i.e., aromaticity) (Alberts and Takács 2004), since a higher degree of molecular conjugation and the resulting intramolecular reabsorption of the emitted fluorescence causes redshift of fluorescence peaks (Peuravuori et al. 2002) [see Fig. 1 in Supplementary Information (SI) for further discussion of the characteristics of peaks A and C and comparison with literature values].

Classical fluorescence indices

FI, BIX and HIX are commonly used to indicate DOM sources, the freshness of DOM components and DOM age, respectively. In our study, for example, the FI value ranged from 0.7 [DHA, Dando soil humic acid (HA)] to 1.4 [1R109F, Pony Lake fulvic acid (FA)], suggesting that all the HS standards used in this study are categorized as terrestrially derived humic materials according to the study by McKnight et al. (2001)) (Table 2). BIX for most of our samples (16 of 17 standards) ranged from about 0.3 to 0.6, indicating that these HS samples are likely of allochthonous origin (Birdwell and Engel 2010; Huguet et al. 2009; Wickland et al. 2007). FA from Pony Lake (1R109F) and Biwa Lake (BFZ), however, showed somewhat higher BIX (0.7 and 0.6, respectively), suggesting that FA samples from these lakes consist of a mixture of autochthonous and allochthonous materials. The higher BIX values for lake HS agree with the findings of Birdwell and Engel (2010)) (BIX for Pony Lake = 0.66) and Peng et al. (2014)) (BIX for Pony Lake = 1.0) (Table 2). In addition, HIX for the 17 HS standards ranged from 4.8 to 191. Most of the HS standards (13 of 17 samples) showed HIX values of between 10 and 50, comparable to that of HS isolates (Birdwell and Engel 2010) and DOM from soil and pore water (Kalbitz et al. 2003; Wickland et al. 2007) in the previous studies. The highest HIX value (HIX = 191 for leonardite HA) can be explained by the finding by Birdwell and Engel (2010)) that coal-derived humics have HIX values above 50. Further detailed characteristics of classical fluorescence indices are described further in Table 2.

Indices derived from PARAFAC analysis

PARAFAC analysis was performed by varying the number of components from 3 to 7. The core consistencies were determined to be 86.7, 9.5, −0.73, 0.84 and 0.57 for models with 3, 4, 5, 6 and 7 components, respectively. The 3-component model was considered the best since it provided the highest core consistency. The fluorescence EEM spectral characteristics and the excitation and emission loadings obtained (Fig. 2) were generally similar to those of colored dissolved organic matter (CDOM) in aquatic environments (Cory and McKnight 2005; Stedmon et al. 2003). In addition, most peak positions identified were consistent with the literature, as listed in Table 3. For example, the position of the first peak (P1) is consistent with typical protein-like fluorescence (Fellman et al. 2010), whereas P2, P3, P4 and P5 are consistent with humic-like fluorescence (Coble 1996; Cory and McKnight 2005; Stedmon et al. 2003). The DOM samples used in this study are HS standards, rather than crude DOM samples from natural waters which could include a range of additional organic compounds. It is therefore reasonable that the peak intensity of P1 showed relatively weaker loading compared to the other peaks (Fig. 2). Further, protein-like peaks can be attributed to tryptophan residues present in samples based on information from IHSS (Chen and Kenny 2007).

The fluorescence peaks can be classified into UVA and UVC humic-like fractions based on their excitation wavelength. For example, P2, located at Ex/Em = 350/460 nm, is referred to as the UVA humic-like fraction since the fluorescence intensity at Em 460 nm is a maximum upon absorption of excitation light in the UVA region (Ishii and Boyer 2012). On the other hand, P3 (Ex/Em = 240/444 nm) and P5 (Ex/Em = 270/492 nm) are designated as UVC humic-like fractions because their emission intensity is a maximum, since they absorb light in the UVC region (Ishii and Boyer 2012). The P4 fraction (Ex/Em = 300/444 nm) is a major DOM in oceanic waters (Coble 1996) and is rarely found in river and lake water samples or DOM

from soil. While none of the HS standards used in this study are from marine waters, P4 was statistically selected by PARAFAC analysis. The observed location of P6 is consistent with that reported by Stedmon and Markager (2005b)) (Ex/Em = 420/488 nm). This peak has not yet been defined in the literature. The higher Ex and Em values of P5 and P6 in the third component compared to P3 and P4 in the second component are likely due to the redshift in terrestrial-derived HA.

The fluorescence component contributions (I_n%) were calculated using Eq. 4 (Kowalczuk et al. 2009) to provide quantitative results from the PARAFAC analyses. The contributions of each fluorescence component in the FA and HA groups are shown in Fig. 3. The contributions ranged from 32 to 60% for I_1%, 23–39% for I_2% and 11–27% for I_3%. Component percentages were high for the first and second components for FA than HA ($p = 0.04$ for I_1% and $p = 0.35$ for I_2%), while it was lower for the third component ($p = 5.5 \times 10^{-4}$). Santin et al. (2009)) has reported similar results and addressed the second and the third components as FA-type and HA-type fractions, respectively.

We also determined the relative fluorescence intensity (RF_m) using the PARAFAC-based peak-picking method. The 6 peaks obtained from the 3-component PARAFAC model were used to calculate the relative intensities of the designated peaks using Eq. 5. All 17 HS standards examined in this study provided average values for the relative intensities from 0.08 for RF_6 to 0.25 for RF_3. The higher average RF_1 value for HA compared to FA (Fig. 3) is consistent with the study of Santin et al. (2009)) using HS estuarine soil samples where the tyrosine-like peak intensity for HA was higher than that for FA (Ex/Em = 275/304 nm, $p = 0.02$). RF_3 and RF_4, located at Ex/Em = 240/444 nm and Ex/Em = 300/444 nm, respectively, had higher values for FA than for HA ($p = 1.4 \times 10^{-5}$ for RF_3 and $p = 1.8 \times 10^{-3}$ for RF_4). Consistent with this result, Santin et al. (2009)) characterized both these fluorescence components as FA-type components (e.g., Ex/Em: 260/439 and 305/439 nm). In contrast, RF_5 and RF_6 had higher HA than FA values ($p = 0.017$ for RF_5 and $p = 2.9 \times 10^{-4}$ for RF_6). Santin et al. (2009)) and He et al. (2006)) reported that the component in the Ex/Em range comparable to RF_5 was designated as an HA-type fraction because HA dominates these fluorescence components. However, neither of these previous studies observed a peak located in a range comparable to P6.

Relationship between optical parameters and the molecular composition of HS

Several previous studies have linked optical characteristics of DOM to compositional parameters (Belzile and Guo

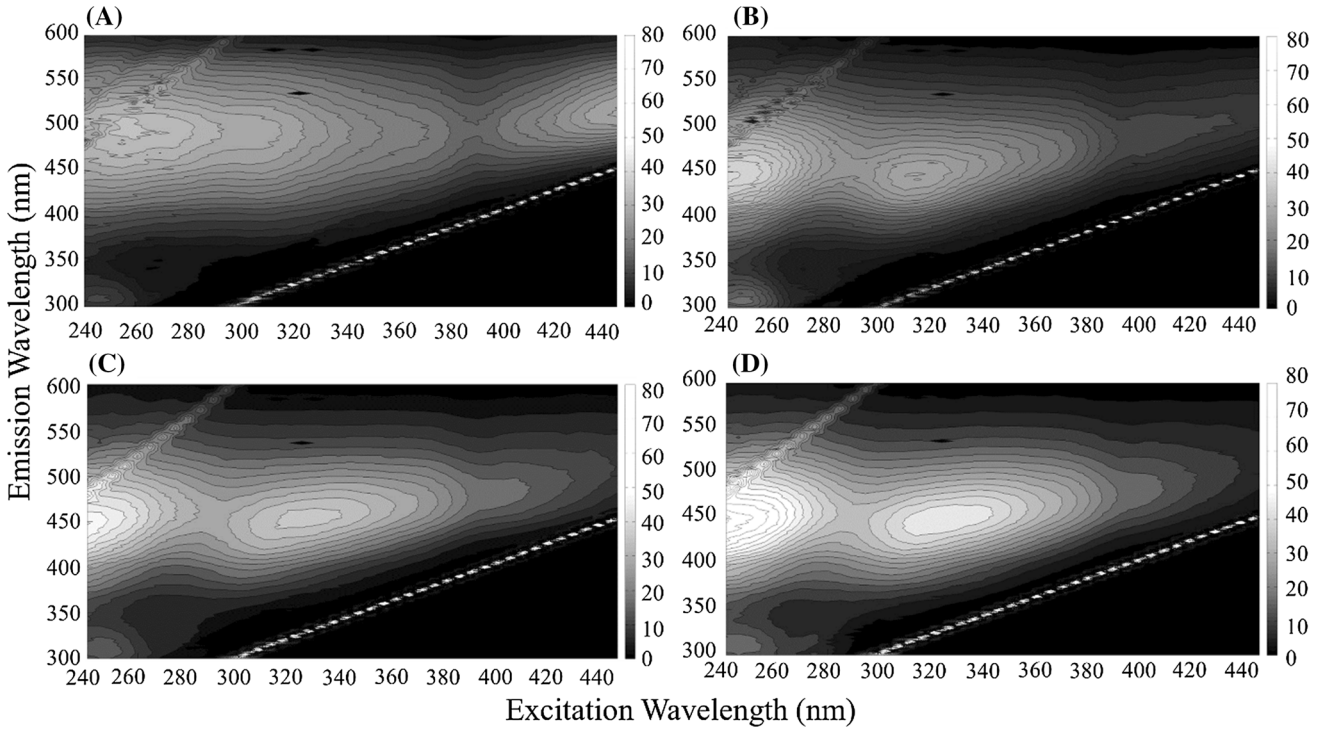

Fig. 1 EEM contours of standard humic substances in four different sources: **a** Elliott Soil HA (1S102H), **b** Suwannee River HA (2S101H), **c** Nordic Lake FA (1R105F) and **d** Suwanne River FA (1S101F)

Table 2 Comparison of peak positions and fluorescence indices in this study to literature

	Sample origin	Ex/Em pairs			Fluorescence indices	
		Peak A	Peak C	FI	BIX	HIX
FA	Nordic Lake	**240/448**	**325/452**	**1.1**	**0.38**	**16.97**
		335/447	335/461[a]	0.99[b]		10–50[d]
		230/436	335/461[b]			
	Pony Lake	**240/426**	**305/420**	**1.43**	**0.71**	**8.42**
				1.51[d]	0.66[d]	10–50[d]
				1.46[f]		
				1.93[g]	1[g]	6.87[g]
	Suwanne River I	**240/452**	**325/448**	**1.18**	**0.41**	**17.09**
		229/432	332/442[a]	1.44[b]		10–50[d]
		230/437	335/457[b]	1.31[f]		
		255/455	320/450[c]	1.29[g]	0.54[g]	14.27[h]
	Suwanne River II	**240/450**	**320/448**	**1.13**	**0.37**	**20.04**
				1.3[e]		10–50[d]
	Pahokee Peat II	**240446**	**320/448**	**1.01**	**0.31**	**81.75**
		230/433	323/437[a]			10–50[d]
	Inogashira Soil	**240/444**	**315/442**	**1.21**	**0.37**	**26.42**
	Dado Soil	**240/440**	**315/442**	**1.1**	**0.36**	**15.99**
	Biwa Lake	**240/436**	**310/428**	**1.28**	**0.6**	**4.83**
HA	Pahokee Peat II	**250/474**	**440/522**	**0.84**	**0.38**	**30.22**
						10–50[d]
	Nordic Lake	**240/436**	**315/442**	**1.01**	**0.36**	**10.04**
		232/435	333/450[a]			10–50[d]
	Waskish Peat	**245/450**	**315/448**	**0.96**	**0.4**	**14.41**
						10–50[d]
	Elliott Soil	**260/494**	**440/518**	**0.82**	**0.37**	**30.89**
		278/464	459/513[a]	1.15[e]		10–50[d]
		270/550	360/560[c]			
	Pahokee Peat II	**250/486**	**440/524**	**0.81**	**0.37**	**30.92**
		268/465	456/513[a]			10–50[d]
	Leonardite	**255/486**	**440/518**	**0.88**	**0.4**	**191.3**
		265/458	454/511[a]			>50[d]
	Suwannee River II	**240/444**	**315/442**	**0.98**	**0.36**	**17.49**
		230/437	335/465[b]	1.19[b]		10–50[d]
		260/485	330/470c	1.08[f]		
	Inogashira Soil	**260/486**	**450/516**	**0.83**	**0.39**	**26.28**
	Dado Soil	**240/442**	**450/510**	**0.69**	**0.47**	**5.14**

[a] Bold numbers indicate fluorescence results in the present study

[b] Alberts and Takács (2004)

[c] Rodríguez et al. (2014)

[d] Sierra et al. (2005)

[e] Birdwell and Engel (2010)

[f] Cory and McKnight (2005)

[g] Korak et al. (2014)

[h] Peng et al. (2014))

2006; Hansell and Carlson 2014). For example, absorbance data have been correlated with several fluorescence parameters and the molecular composition of HS (Alberts and Takács 2004; Weishaar et al. 2003). However, the analyses to date have been fragmentary and comprehensive investigation on the relationship between the optical

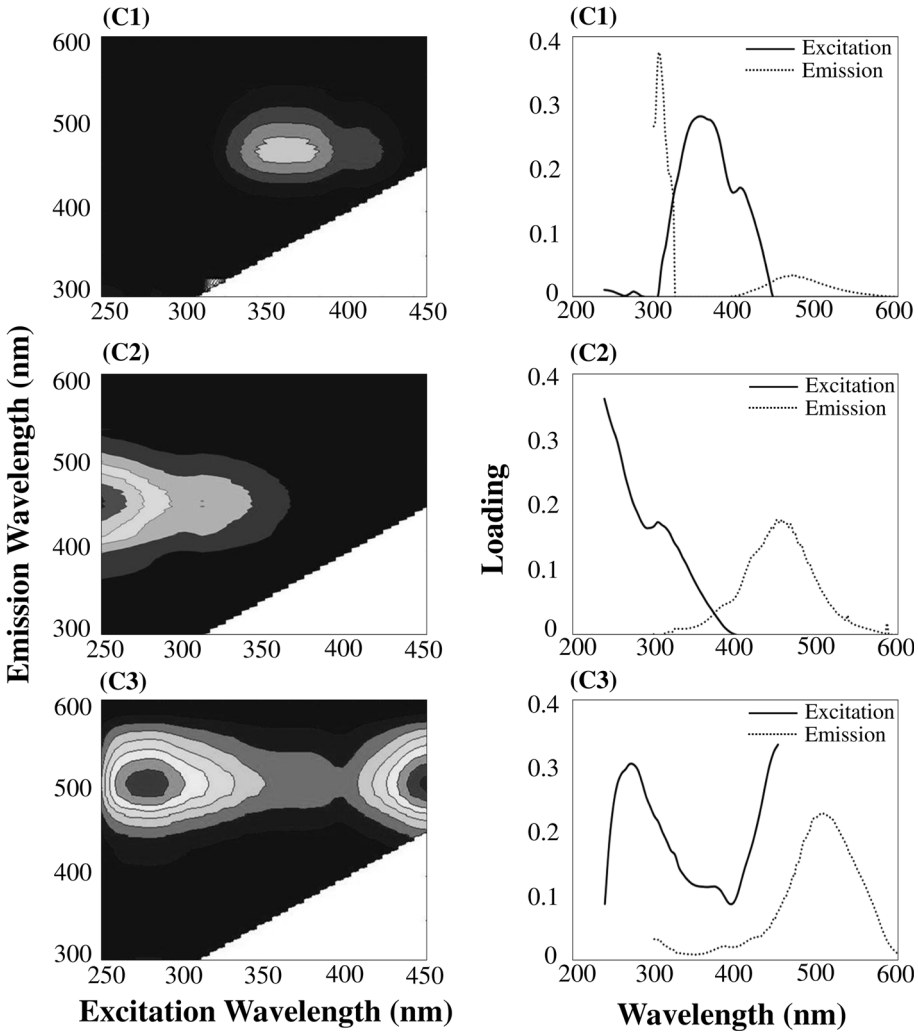

Fig. 2 Contour plots and EEM loadings of the three generated fluorescence components

properties and molecular composition of DOM has not been provided. Here, CCA and simple correlation analysis were carried out to correlate the HS molecular information and its optical properties using the fluorescence parameters determined in this study (Fig. 4), in addition to UV–Vis absorbance indices, as the optical parameters.

Figure 4 illustrates the biplot from CCA showing the relationship between optical parameters and molecular composition. The first two components cover about 90% of the overall variations. As indicated by the red arrows in Fig. 4, the molecular compositions of HS varied in different directions and contributions. The arrow for the aromatic content was long and had a small angle to the CCA1 axis, suggesting that most of the CCA1 component in the positive direction is accounted for by the degree of aromaticity. Consistent with this, the aliphatic content of HS, which has a negative correlation with the aromatic content, contributed to the CCA1 component in the negative direction. The arrows for the carbohydrate, carbonyl and oxygen atom contents of the CCA2 component were long and had relatively small angles to the CCA2 axis, suggesting that CCA2 represents the O-related structures, including carbohydrate and carbonyls.

Most optical parameters determined here were spread on the CCA1 axis, which is highly associated with the amount of aliphatic and aromatic compounds in HS. For example, I_3%, RF_5, RF_6 and specific ultraviolet absorption ($SUVA_{254}$) are spatially located very close to the arrow representing the amount of aromatic carbon, indicating that these parameters correlate highly with the degree of aromaticity and thus are candidate indicators for the amount of aromatic compound in HS. Indeed, $SUVA_{254}$ is recognized as an indicator of the aromaticity in aqueous systems (Weishaar et al. 2003). In addition, the location of BIX on the axis showing aliphatic content suggests that this index is highly correlated with the amount of aliphatic compound. Other parameters, including E2/E3 (absorbance at 250 nm relative to 365 nm), absorbance slope ($S_{275–295}$), RF_1, RF_3 and RF_4 vary near the CCA1 axis in the negative direction and thus likely correlate with aliphatic and H-rich

Table 3 Six peaks generated from 3 component PARAFAC model in this study and comparison with literature

Component	Peak	Position (Ex/Em, nm)	Common Ex/Em scale (nm)[a,b]	Definition	References[h]
C1	P1	275/306	270-280/300-312	B/T, amino acids, free or bound in proteins	275/300[c]
					275/304[d,g]
					275/306[e]
	P2	350/460	320-360/420-460	C, UVA humic-like fraction (terrestrial)	385/504[d,g]
					370/490[c]
C2	P3	240/444	230-260/400-500	A, UVC humic-like fraction (terrestrial)	240/436[f]
					250/448[d]
	P4	300/444	295-380/374-450	M, marine humic-like fraction	315/418[c]
					325/416[f]
C3	P5	270/492	250-295/478-504	A, UVC humic like	270/478[f]
					260/490[c]
	P6	440/492	Unknown	Undefined but can be found in terrestrial humic acid	420/488[d]

[a] Parlanti et al. (2000)

[b] Coble et al. (1998)

[c] Murphy et al. (2008)

[d] Stedmon and Markager (2005a)

[e] Stedmon and Markager (2005b)

[f] Stedmon et al. (2003)

[g] Santin et al. (2009)

[h] The component number shows the PARAFAC number in specific literature

compounds. These results are consistent with the simple correlation analysis, which indicates the high correlation coefficients between the amount of aliphatic carbon and BIX ($r = 0.84$, $p = 7.8 \times 10^{-5}$) and between the amount of aromatic carbon and other optical parameters including FI ($r = 0.78$, $p = 6.6 \times 10^{-4}$), I_3% ($r = 0.85$, $p = 1.6 \times 10^{-3}$), RF_5 ($r = 0.80$, $p = 3.8 \times 10^{-4}$), E2/E3 ($r = 0.71$, $p = 3.2 \times 10^{-3}$) and RF_6 ($r = 0.80$, $p = 3.3 \times 10^{-4}$) (Table 1). Several other chemical classes, such as sulfur-containing compounds, have a longer axis, but no optical parameters appear close to this axis, suggesting that optical parameters may be unsuitable for estimating the sulfur-compound content of HS.

The correlation analysis between single molecular and fluorescence parameters indicated that the fluorescence properties of HS, including the PARAFAC component contribution, significantly correlate well with the other parameters related to HS molecular composition (e.g., the elemental composition, carbon species, acidic functional group content and iron complexation parameters) (Table 4). For example, I_3% showed significant correlations ($p < 0.05$) with elemental composition (O and N) and carbohydrate content, while $SUVA_{254}$ had high correlation with carboxyl content. Fe(III) complexation is one of the important functions of HS in natural aquatic environments, and thus, the correlations between HS optical parameters and Fe(III) complexation parameters (complexation capacity (C_{Fe}) and stability constant (K_{Fe}) at pH 8.0] were examined. As shown in Table 4, Fe(III) complexation parameters were correlated with FI, I_3%, RF_3 and RF_6. These selected optical parameters are correlated highly with aromaticity (Table 4). Previous work by Fujii et al. (2014)) consistently indicated that specific functional groups, including those located near aromatic groups in HS, are likely preferable for Fe(III) coordination at circumneutral pH. In addition, the result agrees overall with the view put forth by McKnight et al. (2001)) that FI is likely to be a useful tool for estimating metal-FA complexation in natural waters. Comparison of the correlation coefficients indicated that RF_6 has the highest correlation to the Fe(III) binding parameters, perhaps, because RF_6 can effectively quantify the redshift caused by condensed aromatic rings and other unsaturated bonding structures likely associated, either directly or indirectly, with the Fe(III) binding properties of HS (Fujii et al. 2014). However, the present results do not necessarily exclude

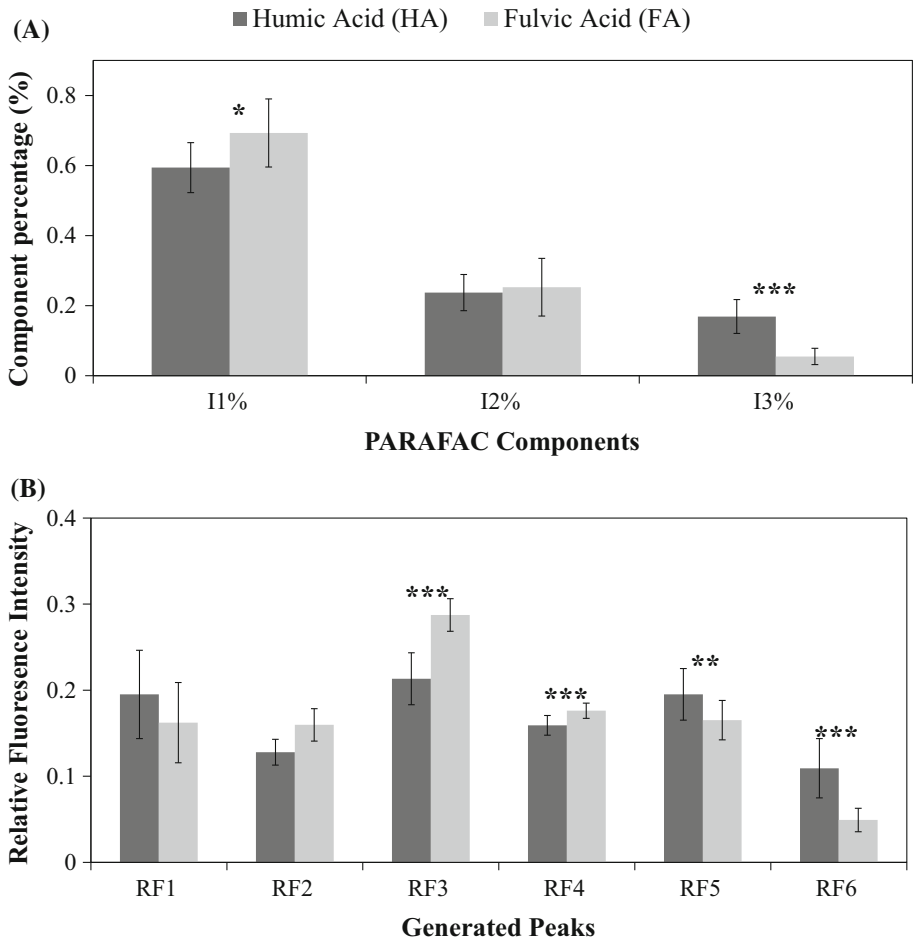

Fig. 3 **a** Average fluorescence component contributions (I_n%) of the 3 PARAFAC components for fulvic and humic acid fractions. Standard deviations of all samples are shown. **b** Average fluorescence relative intensities (RF_m) of 6 peaks generated from PARAFAC modeling for fulvic and humic acid fractions. Standard deviations of all samples are shown. *Asterisks* represent statistically significant levels (*$p < 0.05$; **$p < 0.01$; ***$p < 0.001$)

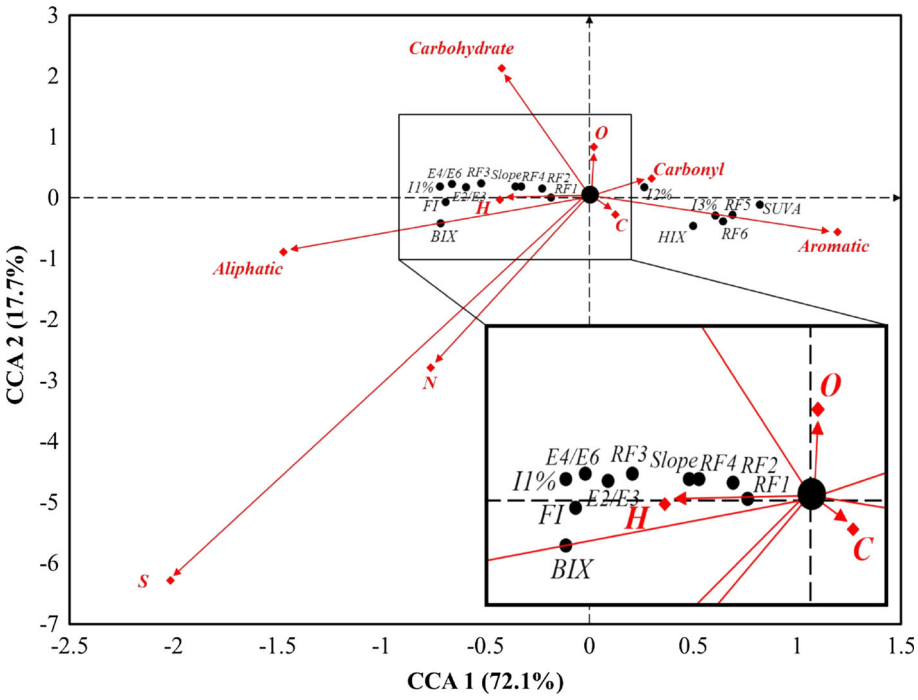

Fig. 4 Canonical correspondence analysis for characterization of the relationship between the molecular composition and optical parameters of humic substances. 72.1% of variance is explained by the first component CCA axis 1, while 17.7% of variance is explained by the second component CCA axis 2

Table 4 Correlation coefficients between fluorescence parameters and chemical properties of humic substances

Fluorescence Parameters	Elemental composition (%)					Atomic ratio			Carbon species from ^{13}C NMR (%)				Aromaticity	Acidic functional groups (meg/g)		Fe(III) Complexation parameters[f]	
	C	H	O	N	S	O/C	N/C	H/C	Aliphatic	Carbohydrate	Aromatic	Carbonyl		Carboxyl	Phenolic	K_{FeL}	C_{FeL}
Classical indices																	
FI[a]	−0.46	0.36	0.26	−0.14	0.37	0.34	−0.09	**0.51**	**0.68****	0.04	**−0.78*****	0.20	**−0.71****	0.43	−0.18	**−0.64****	**−0.65****
BIX[b]	0.06	*0.82****	**−0.51***	**0.58***	*0.66***	−0.37	**0.61***	**0.77*****	*0.84****	−0.08	**−0.61***	−0.48	**−0.65****	−0.20	0.17	−0.34	−0.36
HIX[c]	**0.60***	−0.33	−0.33	−0.16	0.04	−0.38	−0.19	**−0.56***	−0.36	**−0.59***	**0.62***	0.03	**0.59***	0.09	−0.30	**0.67****	0.48
Component contribution[d]																	
I_1%	−0.41	**0.52**	**0.50**	**−0.54**	−0.24	0.37	**−0.54**	**0.64***	**0.57**	*0.63*	**−0.72***	0.26	**−0.69***	*−0.04*	0.22	**−0.62**	−0.38
I_2%	−0.22	−0.48	0.21	−0.13	−0.23	0.33	−0.06	−0.15	−0.11	−0.27	0.16	0.03	0.16	0.48	−0.32	0.07	−0.16
I_3%	**0.76****	−0.28	*−0.85****	*0.84****	**0.53**	*−0.79****	*0.79****	**−0.77****	**−0.70***	*−0.63*	**0.85****	−0.39	**0.82****	−0.46	0.02	**0.81****	**0.69***
Relative fluorescence intensity[e]																	
RF_1	0.09	**0.64****	−0.26	0.30	0.10	−0.26	0.30	**0.59***	0.23	0.36	−0.23	−0.39	−0.28	**−0.62***	0.33	−0.32	−0.10
RF_2	−0.28	−0.10	0.37	−0.48	0.23	0.32	−0.45	−0.05	0.25	−0.04	−0.40	0.46	−0.31	0.46	−0.28	−0.34	−0.33
RF_3	*−0.76****	0.10	**0.69****	−0.48	−0.01	**0.74****	−0.41	0.36	0.42	0.29	**−0.68****	0.31	**−0.60***	**0.81****	−0.26	**−0.72****	**−0.73****
RF_4	**−0.60***	−0.03	0.49	−0.30	0.03	**0.58***	−0.24	0.14	0.28	0.14	−0.44	0.21	−0.39	**0.75****	−0.14	−0.33	**−0.57***
RF_5	**0.54***	**−0.56***	−0.35	0.20	−0.18	−0.38	0.14	**−0.72****	**−0.59***	−0.44	**0.80*****	−0.03	**0.75****	0.03	−0.08	**0.84*****	**0.69****
RF_6	**0.70****	−0.34	**−0.59***	0.42	−0.02	**−0.62***	0.35	**−0.57***	**−0.52***	−0.44	**0.80*****	−0.20	**0.74****	−0.45	0.13	*0.85****	*0.79****
$SUVA^{g}_{254}$	**0.55***	**−0.63****	−0.26	0.00	−0.39	−0.36	−0.06	*−0.82****	**−0.76*****	−0.32	*0.88****	0.06	*0.85****	*−0.86****	−0.05	**0.80*****	**0.69****
$S^{h}_{275–295}$	**−0.65****	0.39	0.45	−0.18	0.03	**0.56***	−0.11	**0.62***	**0.58***	0.27	**−0.76****	0.12	**−0.71****	**0.60***	0.00	**−0.72****	**−0.65****
E2/E3[i]	**−0.67****	0.31	0.49	0.21	−0.04	**0.60***	−0.14	0.55*	**0.52***	0.26	**−0.71****	0.17	**−0.65****	**0.64***	0.00	**−0.67****	**−0.63***
E4/E6[j]	−0.30	**0.64****	0.19	0.25	−0.00	0.22	−0.21	**0.71****	**0.58***	0.38	**−0.77*****	0.04	**−0.73****	0.52	−0.14	**−0.71****	**−0.59***

Bold characters and italic highlight indicate correlation coefficient: $r > 0.50$ and the highest significant correlation, respectively. (* $p < 0.05$; ** $p < 0.01$; *** $p < 0.001$)

[a] McKnight et al. (2001)

[b] Huguet et al. (2009)

[c] Zsolnay et al. (1999)

[d] Kowalczuk et al. (2009))

[e] Indices developed in the present study (e.g., $RF_1 = P_1/(P_1 + P_2 + P_3 + P_4 + P_5 + P_6)$

[f] Fujii et al. (2014)), K_{FeL}: stability constant for Fe(III) complexation by humic substances at pH 8.0 (mol l^{-1}); C_{FeL}: binding capacity (mol mg^{-1})

[g] Specific UV absorbance at 254-nm wavelength defined as follows: $SUVA_{254} = A_{254}$/[DOC] where [DOC] represents concentration of dissolved organic carbon (mg L^{-1}) and A_{254} is absorbance at 254-nm wavelength

[h] Spectral slope in the wavelength region of 275–295 nm, which is calculated using linear regression of the natural log-transformed a_λ spectra [$a_\lambda = 2.303A_\lambda/l$; λ: wavelength (in nm); A_λ: absorbance at a wavelength of λ (no unit); l: path length (in m)] (Korshin et al. 2009)

[i] E2/E3: absorbance at 250 nm relative to 365 nm

[j] E4/E6: absorbance at 465 nm relative to 665

the importance of other structures in metal binding by HS (e.g., aliphatic carboxyl in close proximity to aromatic structures) (Leenheer et al. 1998; Manceau and Matynia 2010).

Finally, the statistical results obtained in this study allowed us to establish a series of empirical equations describing the substantial relationship between fluorescence parameters and HS chemical properties (Table S1 in SI).

Conclusion

In conclusion, we comprehensively analyzed the relationship between optical properties (e.g., FI, BIX, HIX and PARAFAC-derived parameters) and molecular composition for chemically well-defined HS standards. Our findings generally indicated that such fluorescence properties of HS significantly correlate well with several aspects of the molecular composition of HS including aromaticity, elemental composition, carbon species, acidic functional group content and iron complexation. These results suggest that the measurement of HS fluorescence is useful in understanding the molecular composition and environmental functions of DOM in natural environments.

Acknowledgements We appreciate the financial supports from JST CREST and JSPS Young Scientists (A) (Grant Number: 25709045). The financial support from the Ministry of Environment, Japan (Environment Research and Technology Development Fund) (Grant Number: S-13-2-3) is also appreciated.

References

Aiken GR (1985) Humic substances in soil, sediment, and water: geochemistry, isolation, and characterization. Wiley, New York

Alberts JJ, Takács M (2004) Total luminescence spectra of IHSS standard and reference fulvic acids, humic acids and natural organic matter: comparison of aquatic and terrestrial source terms. Org Geochem 35:243–256

Alberts JJ, Takács M, Egeberg PK (2002) Total luminescence spectral characteristics of natural organic matter (NOM) size fractions as defined by ultrafiltration and high performance size exclusion chromatography (HPSEC). Org Geochem 33:817–828

Baghoth S, Sharma S, Amy G (2011) Tracking natural organic matter (NOM) in a drinking water treatment plant using fluorescence excitation–emission matrices and PARAFAC. Water Res 45:797–809

Belzile C, Guo L (2006) Optical properties of low molecular weight and colloidal organic matter: application of the ultrafiltration permeation model to DOM absorption and fluorescence. Mar Chem 98:183–196

Birdwell JE, Engel AS (2010) Characterization of dissolved organic matter in cave and spring waters using UV–Vis absorbance and fluorescence spectroscopy. Org Geochem 41:270–280

Bukaveckas PA, Robbins-Forbes M (2000) Role of dissolved organic carbon in the attenuation of photosynthetically active and ultraviolet radiation in Adirondack lakes. Freshw Biol 43:339–354

Campitelli PA, Velasco MI, Ceppi SB (2006) Chemical and physicochemical characteristics of humic acids extracted from compost, soil and amended soil. Talanta 69:1234–1239

Carstea EM, Baker A, Bieroza M, Reynolds DM, Bridgeman J (2014) Characterisation of dissolved organic matter fluorescence properties by PARAFAC analysis and thermal quenching. Water Res 61:152–161

Chen H, Kenny JE (2007) A study of ph effects on humic substances using chemometric analysis of excitation-emission matrices. Ann Environ Sci 1:1–9

Chin Y-P, Aiken G, O'Loughlin E (1994) Molecular weight, polydispersity, and spectroscopic properties of aquatic humic substances. Environ Sci Technol 28:1853–1858

Coble PG (1996) Characterization of marine and terrestrial DOM in seawater using excitation-emission matrix spectroscopy. Mar Chem 51:325–346

Coble PG, Del Castillo CE, Avril B (1998) Distribution and optical properties of CDOM in the Arabian Sea during the 1995 Southwest Monsoon. Deep Sea Res Part II 45:2195–2223

Cory RM, McKnight DM (2005) Fluorescence spectroscopy reveals ubiquitous presence of oxidized and reduced quinones in dissolved organic matter. Environ Sci Technol 39:8142–8149

Fellman JB, Hood E, Spencer RG (2010) Fluorescence spectroscopy opens new windows into dissolved organic matter dynamics in freshwater ecosystems: a review. Limnol Oceanogr 55:2452–2462

Ferretto N, Tedetti M, Guigue C, Mounier S, Redon R, Goutx M (2014) Identification and quantification of known polycyclic aromatic hydrocarbons and pesticides in complex mixtures using fluorescence excitation–emission matrices and parallel factor analysis. Chemosphere 107:344–353

Fujii M, Imaoka A, Yoshimura C, Waite TD (2014) Effects of molecular composition of natural organic matter on ferric iron complexation at circumneutral pH. Environ Sci Technol 48:4414–4424

Fujitake N, Kodama H, Nagao S, Tsuda K, Yonebayashi K (2009) Chemical properties of aquatic fulvic acids isolated from Lake Biwa, a clear water system in Japan. Hum Subst Res 5:1

Hansell DA, Carlson CA (2014) Biogeochemistry of marine dissolved organic matter. Chapter 10—The Optical Properties of DOM in the Ocean. Academic Press,

He Z, Ohno T, Cade-Menun BJ, Erich MS, Honeycutt CW (2006) Spectral and chemical characterization of phosphates associated with humic substances. Soil Sci Soc Am J 70:1741–1751

Hertkorn N et al (2006) Characterization of a major refractory component of marine dissolved organic matter. Geochim Cosmochim Acta 70:2990–3010

Huguet A, Vacher L, Relexans S, Saubusse S, Froidefond J-M, Parlanti E (2009) Properties of fluorescent dissolved organic matter in the Gironde Estuary. Org Geochem 40:706–719

Ishii SK, Boyer TH (2012) Behavior of reoccurring PARAFAC components in fluorescent dissolved organic matter in natural and engineered systems: a critical review. Environ Sci Technol 46:2006–2017

Jaffé R, McKnight D, Maie N, Cory R, McDowell W, Campbell J (2008) Spatial and temporal variations in DOM composition in ecosystems: the importance of long-term monitoring of optical properties. J Geophys Res Biogeosci 2005–2012:113

Kalbitz K, Schmerwitz J, Schwesig D, Matzner E (2003) Biodegradation of soil-derived dissolved organic matter as related to its properties. Geoderma 113:273–291

Korak JA, Dotson AD, Summers RS, Rosario-Ortiz FL (2014) Critical analysis of commonly used fluorescence metrics to characterize dissolved organic matter. Water Res 49:327–338

Korshin G, Chow CW, Fabris R, Drikas M (2009) Absorbance spectroscopy-based examination of effects of coagulation on the reactivity of fractions of natural organic matter with varying apparent molecular weights. Water Res 43:1541–1548

Kowalczuk P, Durako MJ, Young H, Kahn AE, Cooper WJ, Gonsior M (2009) Characterization of dissolved organic matter fluorescence in the South Atlantic Bight with use of PARAFAC model: interannual variability. Mar Chem 113:182–196

Leenheer J, Brown G, MacCarthy P, Cabaniss S (1998) Models of metal binding structures in fulvic acid from the Suwannee River. Ga Environ Sci Technol 32:2410–2416

Manceau A, Matynia A (2010) The nature of Cu bonding to natural organic matter. Geochim Cosmochim Acta 74:2556–2580

McKnight DM, Boyer EW, Westerhoff PK, Doran PT, Kulbe T, Andersen DT (2001) Spectrofluorometric characterization of dissolved organic matter for indication of precursor organic material and aromaticity. Limnol Oceanogr 46:38–48

Minor E, Stephens B (2008) Dissolved organic matter characteristics within the Lake Superior watershed. Org Geochem 39:1489–1501

Murphy KR, Stedmon CA, Waite TD, Ruiz GM (2008) Distinguishing between terrestrial and autochthonous organic matter sources in marine environments using fluorescence spectroscopy. Mar Chem 108:40–58

Murphy KR, Butler KD, Spencer RG, Stedmon CA, Boehme JR, Aiken GR (2010) Measurement of dissolved organic matter fluorescence in aquatic environments: an interlaboratory comparison. Environ Sci Technol 44:9405–9412

Parlanti E, Wörz K, Geoffroy L, Lamotte M (2000) Dissolved organic matter fluorescence spectroscopy as a tool to estimate biological activity in a coastal zone submitted to anthropogenic inputs. Org Geochem 31:1765–1781

Peiris R, Budman H, Moresoli C, Legge R (2011) Identification of humic acid-like and fulvic acid-like natural organic matter in river water using fluorescence spectroscopy. Water Sci Technol 63(10):2427–2433

Peng N, Wang K, Liu G, Li F, Yao K, Lv W (2014) Quantifying interactions between propranolol and dissolved organic matter (DOM) from different sources using fluorescence spectroscopy. Environ Sci Pollut Res 21:5217–5226

Peuravuori J, Koivikko R, Pihlaja K (2002) Characterization, differentiation and classification of aquatic humic matter separated with different sorbents: synchronous scanning fluorescence spectroscopy. Water Res 36:4552–4562

Piccolo A (2001) The supramolecular structure of humic substances. Soil Sci 166:810–832

Rodríguez FJ, Schlenger P, García-Valverde M (2014) A comprehensive structural evaluation of humic substances using several fluorescence techniques before and after ozonation. Part I: Structural characterization of humic substances. Sci Total Environ 476:718–730

Santin C, Yamashita Y, Otero X, Alvarez M, Jaffé R (2009) Characterizing humic substances from estuarine soils and sediments by excitation-emission matrix spectroscopy and parallel factor analysis. Biogeochemistry 96:131–147

Schindler DW, Curtis PJ, Parker BR, Stainton MP (1996) Consequences of climate warming and lake acidification for UV-B penetration in North American boreal lakes. Nature 379(6567):705–708

Schmidt F, Elvert M, Koch BP, Witt M, Hinrichs K-U (2009) Molecular characterization of dissolved organic matter in pore water of continental shelf sediments. Geochim Cosmochim Acta 73:3337–3358

Scott DT, McKnight DM, Blunt-Harris EL, Kolesar SE, Lovley DR (1998) Quinone moieties act as electron acceptors in the reduction of humic substances by humics-reducing microorganisms. Environ Sci Technol 32:2984–2989

Scully NM, Cooper WJ, Tranvik LJ (2003) Photochemical effects on microbial activity in natural waters: the interaction of reactive oxygen species and dissolved organic matter. FEMS Microbiol Ecol 46:353–357

Sierra M, Giovanela M, Parlanti E, Soriano-Sierra E (2005) Fluorescence fingerprint of fulvic and humic acids from varied origins as viewed by single-scan and excitation/emission matrix techniques. Chemosphere 58:715–733

Stedmon CA, Bro R (2008) Characterizing dissolved organic matter fluorescence with parallel factor analysis: a tutorial. Limnol Oceanogr Methods 6:572–579

Stedmon CA, Markager S (2005a) Resolving the variability in dissolved organic matter fluorescence in a temperate estuary and its catchment using PARAFAC analysis. Limnol Oceanogr 50:686–697

Stedmon CA, Markager S (2005b) Tracing the production and degradation of autochthonous fractions of dissolved organic matter by fluorescence analysis. Limnol Oceanogr 50:1415–1426

Stedmon CA, Markager S, Bro R (2003) Tracing dissolved organic matter in aquatic environments using a new approach to fluorescence spectroscopy. Mar Chem 82:239–254

Stedmon CA, Thomas DN, Granskog M, Kaartokallio H, Papadimitriou S, Kuosa H (2007) Characteristics of dissolved organic matter in Baltic coastal sea ice: allochthonous or autochthonous origins? Environ Sci Technol 41:7273–7279

Sundman A, Karlsson T, Persson P (2013) An experimental protocol for structural characterization of Fe in dilute natural waters. Environ Sci Technol 47:8557–8564

Tipping E, Rey-Castro C, Bryan SE, Hamilton-Taylor J (2002) Al (III) and Fe(III) binding by humic substances in freshwaters, and implications for trace metal speciation. Geochim Cosmochim Acta 66:3211–3224

Watanabe A, Itoh K, Arai S, Kuwatsuka S (1994) Comparison of the composition of humic and fulvic acids prepared by the IHSS method and NAGOYA method. Soil science and plant nutrition 40:601–608

Weishaar JL, Aiken GR, Bergamaschi BA, Fram MS, Fujii R, Mopper K (2003) Evaluation of specific ultraviolet absorbance

as an indicator of the chemical composition and reactivity of dissolved organic carbon. Environ Sci Technol 37:4702–4708

Wickland KP, Neff JC, Aiken GR (2007) Dissolved organic carbon in Alaskan boreal forest: sources, chemical characteristics, and biodegradability. Ecosystems 10:1323–1340

Zsolnay A, Baigar E, Jimenez M, Steinweg B, Saccomandi F (1999) Differentiating with fluorescence spectroscopy the sources of dissolved organic matter in soils subjected to drying. Chemosphere 38:45–50